THE JOURNAL OF BIOLOGICAL CHEMISTRY VOL. 285, NO. 40, pp. 31055–31065, October 1, 2010

Foxo1, a Novel Regulator of Osteoblast Differentiation and Skeletogenesis*

Received for publication, October 29, 2009, and in revised form, June 16, 2010 Published, JBC Papers in Press, July 22, 2010, DOI 10.1074/jbc.M109.079962

Cristina C. Teixeira[‡§], **Yuexun Liu**[‡], **Lwin M. Thant**[§], **Jason Pang**[§], **Glyn Palmer**[§], **and Mani Alikhani**[‡1]

From the Departments of [‡]*Orthodontics and* [§]*Basic Science & Craniofacial Biology, New York University College of Dentistry, New York, New York 10010*

Skeletogenesis depends on the activity of bone-forming cells derived from mesenchymal cells. The pathways that control mesenchymal cell differentiation are not well understood. We propose that Foxo1 is an early molecular regulator during mesenchymal cell differentiation into osteoblasts. In mouse embryos, Foxo1 expression is higher in skeletal tissues, while Foxo1 silencing has a drastic impact on skeletogenesis and craniofacial development, specially affecting pre-maxilla, nasal bone, mandible, tibia, and clavicle. Similarly, Foxo1 activity and expression increase in mouse mesenchymal cells under the influence of osteogenic stimulants. In addition, silencing Foxo1 blocks the expression of osteogenic markers such as Runx2, alkaline phosphatase, and osteocalcin and results in decreased culture calcification even in the presence of strong osteogenic stimulants. Conversely, the expression of these markers increases significantly in response to Foxo1 overexpression. One mechanism through which Foxo1 affects mesenchymal cell differentiation into osteoblasts is through regulation of a key osteogenic transcription factor, Runx2. Indeed, our results show that Foxo1 directly interacts with the promoter of Runx2 and regulates its expression. Using a tibia organ culture model, we confirmed that silencing Foxo1 decreases the expression of Runx2 and impairs bone formation. Furthermore, our data reveals that Runx2 and Foxo1 interact with each other and cooperate in the transcriptional regulation of osteoblast markers. In conclusion, our *in vitro*, *ex vivo*, and *in vivo* results strongly support the notion that Foxo1 is an early molecular regulator in the differentiation of mesenchymal cells into osteoblast.

Undifferentiated mesenchymal cells can differentiate into osteoblasts (bone-forming cells), adipocytes (fat cells), chondrocytes (cartilage cells), and myocytes (muscle cells) under the influence of various hormones and growth factors (1). Commitment and differentiation of mesenchymal cells into osteoblasts is crucial during skeletal development and bone growth.

Whether mesenchymal cells differentiate along the osteogenic or other pathway depends on the activation of specific transcription factors. The importance of transcription factors in controlling skeletal development can be appreciated in the human skeletal disorder cleidocranial dysplasia. In this condition, deregulation of an important osteogenic transcription factor, Runx2, produces a striking phenotype with anterior fontanelle, hypoplasia or aplasia of the clavicle, wide pubic symphysis, and short stature (2).

Although some of the transcription factors that control osteoblast differentiation are well characterized, the role of others remains unclear. One such factor is Foxo1 (forkhead box class O). Foxo1 belongs to the winged helix/forkhead family of transcription factors that is characterized by a 100-amino acid monomeric DNA-binding domain called the FOX domain. Other portions of the forkhead proteins, such as the DNA transactivation or DNA transrepression domains, are highly divergent (3). The functions of Foxo1 are dynamically regulated by post-transcriptional modification. Foxo1 is phosphorylated at the three sites: Thr-24, Ser-253, and Ser-316 (4–8). The phosphorylation of Foxo1 leads to its cytoplasmic retention and the inhibition of its transcriptional activity. On the other hand, dephosphorylation localizes Foxo1 to the nucleus, where Foxo1 binds to the forkhead response element in the promoter of target genes and interacts with transcriptional coactivators, resulting in transcriptional regulation (9).

In vitro and *in vivo* studies have shown that FOXO transcription factors control the regulation of many genes involved in fundamental cellular processes, including cell cycle regulation, cell death, modulation of inflammation, metabolism, protection from oxidative stress, and cell survival (10–15). Recently, the role of Foxo1 in differentiation of mesenchymal cells started to unravel. It has been shown that activation of Foxo1 prevents mesenchymal cells from differentiating into fat or muscle cells (16–18). We hypothesize that inhibition of adipogenesis or myogenesis by Foxo1 concurrently signals mesenchymal cells toward osteogenesis. This possibility is supported by the observation that the alkaline phosphatase gene, a marker of osteoblast differentiation, contains a forkhead response element in its promoter (19).

In the present study, we demonstrate that Foxo1 is expressed during skeletogenesis in mouse embryos and that Foxo1 activity increases in the early hours of differentiation of mesenchymal cells into osteoblasts *in vitro*. Silencing Foxo1 significantly disturbs skeletogenesis *in vivo* and *ex vivo* and prevents expression of osteoblast markers and subsequent matrix calcification. In addition, Foxo1 controls Runx2 expression, and can directly interact with this transcription factor, suggesting that Foxo1 induces osteoblast differentiation through regulation and interaction with Runx2. Based on these findings, we propose that

* This work was supported, in whole or in part, by National Institutes of Health Grants 5K08DE017426 and R03DE019499 from NIDCR. This work was also supported by the Muscular Skeletal Repair and Regeneration Center at Hospital for Special Surgery supported by NIH Grant AR046121.

[1] To whom correspondence should be addressed: New York University, College of Dentistry, 345 East 24th St., Rm. 850, New York, NY 10010. Tel.: 212-998-9224; Fax: 212-995-4087; E-mail: mani.alikhani@nyu.edu.

Foxo1 is an early and important regulator of mesenchymal cell differentiation into osteoblasts.

EXPERIMENTAL PROCEDURES

Study Design—The first series of experiments evaluated Foxo1 expression in mouse skeletal tissues at E15.5, a period of active bone formation, by RT-PCR and immunohistochemistry. Foxo1 expression was silenced *in vivo* and *ex vivo* (tibia organ culture) using a lentiviral vector carrying miRNA. The silencing level and specificity were determined by RT-PCR and EMSA, and the impact on bone formation was studied by RT-PCR, histological methods, whole embryo staining, and microCT.[2]

A mouse embryonic cell line treated with the osteogenic stimulants BMP2, SHH, and PTHrP was used to demonstrate that Foxo1 regulates mesenchymal cell differentiation into osteoblasts. Foxo1 expression, protein levels, and activity were measured over time and in parallel with Runx2, alkaline phosphatase, type I collagen (osteoblast markers), and type II collagen (chondrocyte marker). The effect of Foxo1 overexpression and silencing on osteogenic markers such as Runx2, alkaline phosphatase, osteocalcin, and mineral deposition was examined *in vitro* by RT-PCR, ELISA, and biochemical staining. The specificity of the gene silencing was confirmed by RT-PCR, EMSA, ELISA, proliferation, and apoptosis studies. The interaction of Foxo1 with Runx2 was investigated by means of promoter reporter constructs, mutagenesis, EMSA, ChIP assay, RT-PCR, and co-immunoprecipitation studies.

Cell Culture Models—Mouse embryonic C3H10T1/2 cells (ATCC, Manassas, VA) were maintained in Basal Medium Eagle (Sigma-Aldrich) containing 10% fetal bovine serum (FBS) and antibiotics at 37 °C, in a 5% CO_2 atmosphere. The murine osteoblastic cell line, MC3T3-E1, subclone 14(CRL-2549, ATCC) was cultured in alpha modified Minimum Essential Medium (α-MEM) supplemented with 10% FBS, and antibiotics. Osteogenic differentiation was induced using 100 ng/ml BMP2 (Genscript, Piscataway, NJ). In some experiments SHH (500 ng/ml) or PTHrP (10^{-7} M) was added to medium. Calcification studies were performed in presence of ascorbic acid (50 μg/ml) and 10 mM β-glycerophosphate. Alizarin red staining was performed for visualization of calcium deposits. Primary human mesenchymal cells were cultured in α-MEM supplemented with 10% FBS and 10^{-7} M dexamethasone as previously described (20). Cell proliferation was measured by counting cells after fixation and staining with toluidine blue. Apoptosis was measured by detecting cytoplasmic histone-associated DNA (Roche Applied Science).

Foxo1 and Runx2 Activity—Foxo1 and Runx2 activity was measured using an ELISA-based kit (Active Motif, Carlsbad, CA). Briefly, nuclear proteins were extracted, and their protein content was measured (Pierce Protein Assay, ThermoFisher Scientific Inc., Rockford, IL). Nuclear extracts were incubated with immobilized oligonucleotides that bind Foxo1 or Runx2 followed by successive incubations with primary (anti-Runx2 and anti-Foxo1) antibody, horseradish peroxidase-conjugated secondary antibody, and measuring the colorimetric reaction by spectrophotometry. Wild-type consensus oligonucleotides at a higher concentration were used as a specific competitor and mutated consensus oligonucleotides were used as non-competitor.

EMSA—Interactions between nuclear proteins and Foxo1 DNA probe (CAAAACAA) were investigated using an EMSA kit (Panomics Redwood City, CA) following the manufacturer's instructions. Specificity was demonstrated for each reaction by adding 100-fold molar excess of unlabeled competitive oligonucleotide or unlabeled nonspecific oligonucleotide. Three potential Foxo1 DNA binding sites were identified in the Runx2 promoter using Biobase (Biobase, Biological Databases, Beverly, MA) and three unlabeled oligonucleotides corresponding to these sites were created: synthetic probe A: CCATTATAAACAACAAAAACTTACAGTTTC (−1204 to −1233), synthetic probe B, AGAATTATACAAAACATTTTCTTTGAAAAGAT (−1071 to −1100), and synthetic probe C, CCTGACATTTGTTTTTTAAGATCTTCAAAG (−986 to −1015). In some experiments nuclear proteins were incubated with a 100-fold excess of unlabeled probes A, B, and C.

Silencing Foxo1 in Vitro Using siRNA—C3H10T1/2 cells were incubated with Foxo1 siRNA or scrambled siRNA mixed with HiPerFect Reagent (Qiagen, Valencia, CA) following the manufacturer's protocol. For calcification study, cells were incubated with Foxo1 siRNA (or scrambled siRNA) once a week and stimulated with BMP2 for 14 days.

Foxo1 Overexpression and Runx2 Promoter Studies—C3H10T1/2 cells were transfected with Lipofectamine2000 (Invitrogen, Carlsbad, CA) following the manufacturer's protocol with pcDNA3 Flag Foxo1 (Addgene, Cambridge, MA) or pcDNA3.1 as a control. Transfection efficiency was determined using pcDNA3-EGFP (Addgene, Cambridge, MA), and Foxo1 protein levels were evaluated by Western blot using polyclonal antisera against Foxo1 (Cell Signaling Technology, Danvers, MA). Runx2 promoter activity was determined using a pGL4.10 firefly luciferase reporter plasmid (Promega, Madison, WI) containing two different fragments of the mouse Runx2 promoter region (−0.9 kb or −1.3 kb upstream of transcription starting site), and pGL4.74 basic plasmid (*Renilla* luciferase) for control of transfection efficiency. In some experiments a mutation was introduced in potential binding sites of Foxo1 in the Runx2 promoter. Cells were harvested 24 h post-transfection and tested using a luciferase assay system (Dual-Glo, Promega, Madison, WI) and a Synergy HT Multi-Mode Microplate Reader (BioTek, Winooski, VT). Data were expressed as the ratio of experimental sample's luminescence/control luciferase luminescence.

RT-PCR—Expression of alkaline phosphatase (ALP), osteocalcin, type I and type II collagen, Foxo1, Foxo3, Foxo4, and Runx2 was analyzed by semiquantitative real-time RT-PCR. mRNA was isolated using the RNeasy Kit, and RT-PCR was conducted using the QuantiTect SYBR Green RT-PCR kit (Qiagen) on a DNA Engine Optican 2 System (MJ Research, Waltham, MA). Specific primers for these genes were designed using the murine sequences and for GAPDH as a reference "housekeeping gene" for quantification. Relative expression

[2] The abbreviations used are: microCT, micro computed tomography; SHH, sonic hedgehog; PTHr, parathyroid hormone-related peptide; ALP, alkaline phosphatase; miRNA, microRNA.

levels are reported as "-fold change" (x in the following formula) in gene expression and calculated using the threshold cycle (C_t) and the following formula, in which ctl = control, exp = experimental, and GAPDH = the housekeeping gene: $x = 2^{\Delta\Delta C_t}$, where $\Delta\Delta C_t = \Delta E - \Delta C$, $\Delta E = C_{texp} - C_{tGAPDH}$, and $\Delta C = C_{tctl} - C_{tGAPDH}$. The absolute number for $\Delta\Delta C_t$ was used in the calculation, and a negative $\Delta\Delta C_t$ was considered an increase while a positive $\Delta\Delta C_t$ was considered a decrease in gene expression.

ChIP Assay—Formaldehyde (1% final concentration) was added directly to culture medium for 10 min at ambient temperature to cross-link DNA and bound protein. The cells were lysed and sonicated on ice followed by immunoprecipitation overnight with anti-Foxo1 antibody or normal rabbit IgG (Cell Signaling Technology, Danvers, MA), mixed with Protein G Magnetic Beads and collected by centrifugation at 1000 × *g*. Protein-DNA complexes were eluted from the beads followed by a cross-link reversal step. DNA from each immunoprecipitation reaction was examined by semiquantitative PCR. The Foxo1-responsive region of the mouse ALP, osteocalcin, and Runx2 promoters was mapped for primer design using Genomatix Software (Munich, Germany). The specificity of the immunoprecipitation was confirmed by Western blot analysis using antibody against Foxo1 (Cell Signaling Technology, Danvers, MA).

Co-immunoprecipitation and Western Blot Analysis—C3H10T1/2 cells were transfected with pcDNA3 FLAG Foxo1 (Addgene, Cambridge, MA) as described above. BMP2 was added after 24 h (100 ng/ml), and after an additional 48-h nuclear extracts were collected and co-immunoprecipitation performed (Universal Magnetic Co-IP kit, Active Motif, Carlsbad, CA). Briefly, nuclear extracts were combined either with rabbit monoclonal FLAG antibody (Sigma-Aldrich), rabbit polyclonal Runx2 or species matched normal IgG (Santa Cruz Biotechnology, Santa Cruz, CA). Immunoprecipitates were collected with protein G-coated magnetic beads. Co-immunoprecipitation experiments were also conducted with MC3T3-E1 cells treated with BMP2 (100 ng/ml) for 48 h (without transfection). Total nuclear extracts or immunoprecipitates were fractionated by electrophoresis on a 10% SDS-polyacrylamide gel and transferred onto a PVD membrane (polyvinylidene difluoride membrane, Bio-Rad), probed with monoclonal antibodies against either Runx2 or Foxo1, and visualized with horseradish peroxidase-conjugated secondary antibody and chemiluminescence.

Silencing Foxo1 Using miRNA—The tail vein of CD1 timed-pregnant mice (Charles River Laboratories, Wilmington, MA) at E14.5 were injected with lentivirus (pLenti6/V5-DEST, Invitrogen) containing an engineered microRNA (miRNA) for silencing Foxo1 or negative control miRNA (virus titer, 5×10^5 TU/ml). The miRNA insert was designed to target and cleave Foxo1 mRNA. The control miRNA can form a hairpin structure, but does not target any known vertebrate gene.

Skeletal Staining—Embryos were collected at E16.5 for whole embryo staining with alizarin red and Alcian blue. Embryos were dissected and tissues, including tibia, were used to extract mRNA. Embryos were fixed in 70% ethanol overnight, and placed 0.05% alizarin red, 0.015% Alcian blue, 5% acetic acid, in 70% ethanol overnight. Soft tissues were removed by incubation with 1% KOH before storage in glycerol. Digital images of stained bones were analyzed using digital image analysis software (ImageJ, National Institutes of Health) to quantify the area of stained bones.

Organ Culture—For organ culture studies, tibiae were isolated from E15.5 embryos using a stereomicroscope (Nikon, Melville, NY) and allowed to equilibrate overnight in serum-free α-MEM media containing 0.2% bovine serum albumin (BSA), 0.55 mM L-glutamine, 40 units/ml penicillin, and 40 μg/ml streptomycin as described by Serra *et al.* (21). Tibiae were infected with the lentiviral system described above, containing either engineered microRNA for silencing Foxo1, negative control miRNA, or no vector and were kept in culture for 48 h before histological analysis. Experiments were repeated at least 3 times, with 6–9 bones per treatment. Tibiae were also microdissected, to separate the cartilage region (epiphysis) from the region of active bone formation (diaphysis) and RNA or nuclear proteins were extracted for real time RT-PCR or studies of transcription factor activity.

microCT—Embryos were isolated, and tibiae were collected for microCT analysis 48 h post-tail injection, fixed in 4% paraformaldehyde in PBS overnight, and scanned using the Enhanced Vision Systems Model MS-8 *In Vitro* micro computed tomography (microCT) scanner (Amersham Biosciences) at the Imaging Core of the Hospital for Special Surgery (New York, NY). microCT was used to obtain mineral content and density, bone volume fraction, density of bone, and cross-sectional geometry using the instrument's software.

Immunohistochemistry—Embryos were collected from three CD1 timed-pregnant mice (Charles River Laboratories, Wilmington, MA) at E15.5 fixed with 4% paraformaldehyde, embedded in paraffin, and cut into 5-μm sections. Immunohistochemistry staining was performed as previously described (22) using a Vectastain ABC kit (Vector Laboratories, Burlingame, CA) and polyclonal antibody specific for mouse Foxo1 (Santa Cruz Biotechnology, Santa Cruz, CA). Sections were counterstained with Mallory Trichrome stain, mounted, and scanned on Scan Scope G optical microscope (Aperio, Bristol, UK) at 10×. Cultured tibiae were also fixed, embedded in paraffin, and sectioned. Sections were stained with hematoxylin & eosin to visualize cellular structures, Alcian blue to detect cartilage matrix, and von Kossa to detect mineral deposition.

Statistical Analysis—Each experiment was carried out with at least three replicate samples per group, and each experiment was performed three times. Each value represents the mean ± S.D. of three independent experiments ($n = 3$). Significance was tested by non-parametric analysis at the $p < 0.05$ level using the Mann-Whitney test.

RESULTS

Mouse embryonic mesenchymal cells (C3H10T1/2 cells) that have the potential to differentiate into adipocytes, myoblasts, chondroblasts, and osteoblasts were used to study early events in the commitment of mesenchymal cells into osteoblast. These cells differentiate into osteoblasts in response to BMP2 (23, 24), sonic hedgehog (SHH) (25), and parathyroid hormone-related peptide (PTHrP) (26). When mesenchymal cells were treated with BMP2, Foxo1 activity increased 2.5-fold

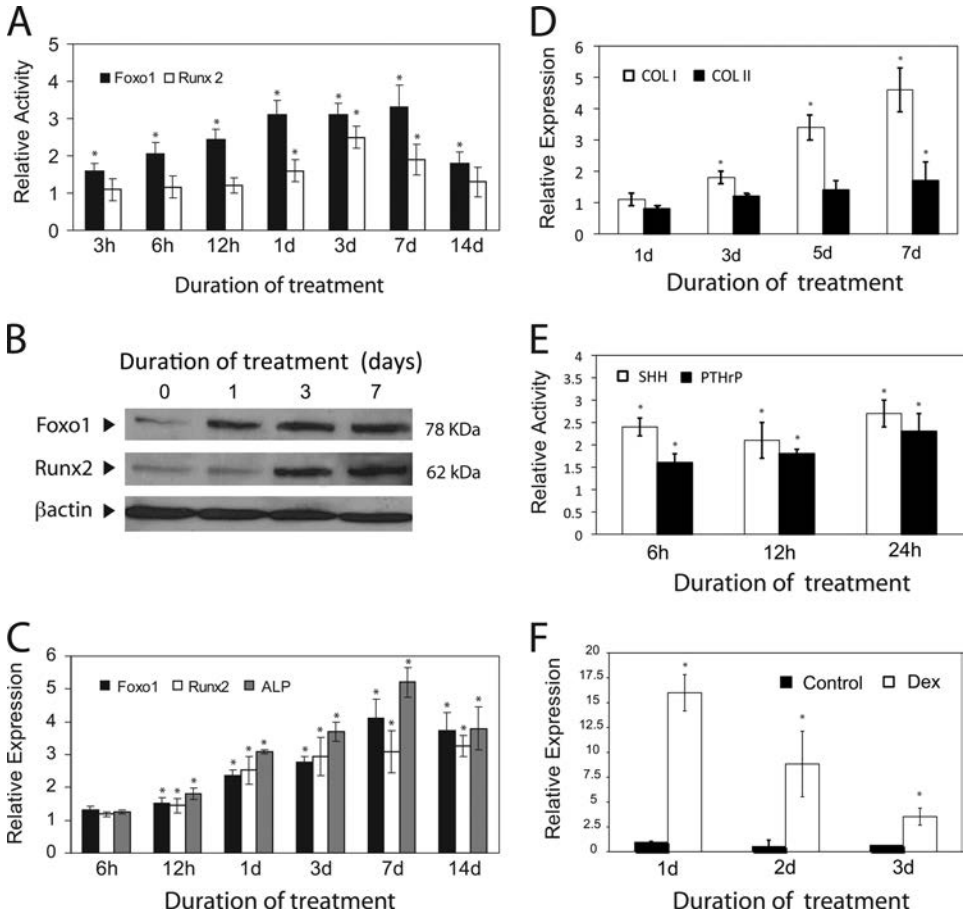

FIGURE 1. **Foxo1 activity and expression increase during osteogenic differentiation.** Mouse mesenchymal cells (C3H10T1/2 cells) were treated with BMP2 (100 ng/ml) to induce osteoblast differentiation. At different time points (h = hours, d = days), cells were collected, and nuclear extracts were isolated and used to measure Foxo1 and Runx2 activities (*A*) and Western blot analysis (*B*). In parallel experiments, mRNA levels for Foxo1, Runx2, and ALP were determined by semiquantitative RT-PCR (*C*). mRNA levels for type I and type II collagen were also measured during the first week in culture (*D*). Foxo1 activity was also determined in nuclear extracts of C3H10T1/2 cells stimulated with SHH (500 ng/ml) and PTHrP (10^{-7} M) (*E*). mRNA levels for Foxo1 in human mesenchyme primary cells stimulated with dexamethasone (10^{-7} M), determined by semiquantitative RT-PCR (*F*). Relative expression values to unstimulated cells are shown. Data are expressed as means ± S.D. of three experiments. *, significantly different from unstimulated cells ($p < 0.05$).

in comparison with cells that did not receive BMP2 after 12 h (Fig. 1*A*), continued to increase in activity after 1, 3, and 7 days, and decreased to 1.8-fold by day 14. The increase in Foxo1 activity relative to control, at all time points studied was statistically significant ($p < 0.05$). Runx2 activity at 3, 6, and 12 h was not statistically significant. Runx2 activity increased to 2.5-fold and 1.9-fold at days 3 and 7, respectively, and these changes were statistically significant ($p < 0.05$). At day 14, Runx2 activity returned to control levels. Similarly Western blotting demonstrates early detection of Foxo1 protein in nuclear extracts of cells treated with BMP2 (Fig. 1*B*).

In cells that were treated with BMP2, Foxo1 expression increased from 1.3-fold at 6 h to 3.7-fold at day 14 with a peak of 4.1-fold at day 7 (Fig. 1*C*). Similar to Foxo1, expression of Runx2 and ALP increased significantly during the time course of study and peaked at 3.1- and 5.2-fold, respectively, at day 7. In addition, a 4.5-fold increase in type I collagen expression ($p < 0.05$) was observed in the first week in culture, while type II collagen expression did not change significantly at the cell densities used in these study (Fig. 1*D*).

Activation and expression of Foxo1 in C3H10T1/2 was not limited to BMP2 stimulation. Similar results were obtained in response to other osteogenic stimulants. SHH and PTHrP increased Foxo1 activity 2.7- and 2.3-fold, respectively, in the first 24 h (Fig. 1*E*). To demonstrate that this phenomenon was not limited to mouse mesenchymal cells, activation of Foxo1 was also measured in primary human mesenchymal cells in response to dexamethasone with similar results (Fig. 1*F*).

Foxo1 expression was down-regulated *in vitro* in both C3H10T1/2 and MC3T3-E1 cells with siRNA to obtain insight into Foxo1 function. This strategy successfully reduced Foxo1 binding activity in MC3T3-E1 cells as demonstrated by EMSA (Fig. 2*A*). Specificity of binding was demonstrated by the competitive inhibition with excess unlabeled probe. Silencing Foxo1 did not affect the expression of other members of the FOXO family, Foxo3, and Foxo4 (Fig. 2*B*), or affect cell proliferation or cell death significantly (Table 1). Foxo1 expression decreased in C3H10T1/2 mesenchymal cells by 76% (Fig. 2*C*). Silencing of Foxo1 expression in mesenchymal cells was able to reduce the up-regulation of Runx2, ALP, and osteocalcin expression in response to BMP2 treatment by 68%, 71%, and 63%, respectively (Fig. 2*C*). Foxo1 silencing also decreased the activity of Foxo1 and Runx 2 by 79 and 62%, respectively (Fig. 2*D*). In addition, cells that were transfected with Foxo1

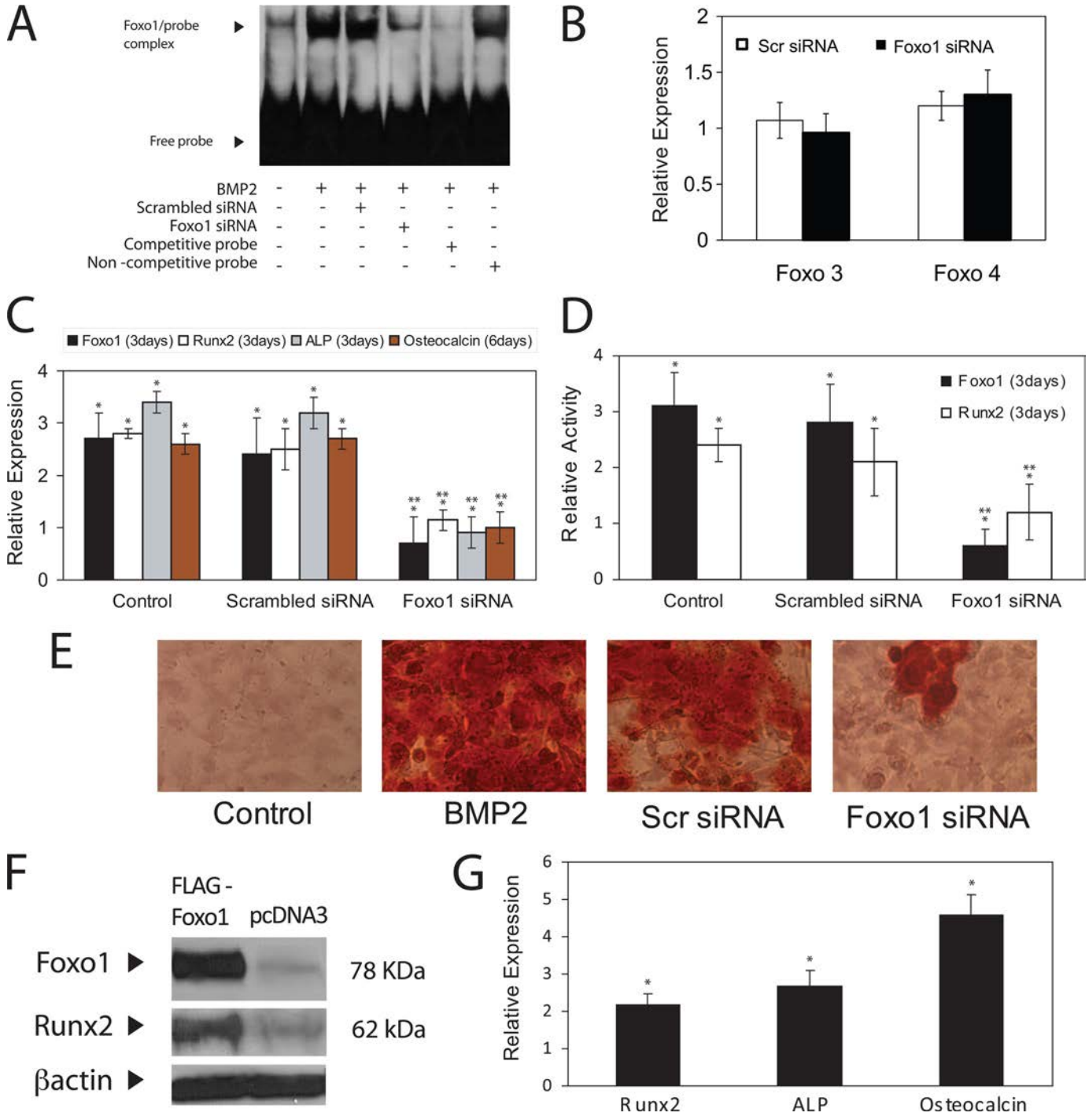

FIGURE 2. **Foxo1 regulates expression of osteogenic markers in differentiating mesenchymal cells.** Activation of Foxo1 was measured by EMSA in MC3T3-E1 cells after transfection with Foxo1 siRNA or scrambled siRNA (48 h) and stimulation with BMP2 for 24 h (*A*). The effect of silencing Foxo1 in the expression of Foxo3 and Foxo4 in C3H10T1/2 cells stimulated with BMP2 (100 ng/ml) (48 h) was determined by semiquantitative RT-PCR (*B*). The proliferation and apoptosis of C3H10T1/2 cells in the same experimental period were also evaluated (Table 2). In similar experiments C3H10T1/2 cells were stimulated with BMP2 and the effect of transfection with Foxo1 siRNA or scrambled siRNA was determined in the expression of Foxo1, Runx2, ALP, and osteocalcin (*C*) and activity of Foxo1 and Runx2 (*D*). Values relative to unstimulated cells are shown. Calcium deposits in these cultures was visualized by alizarin red staining after 14 days in unstimulated cells (*Control*), BMP-treated cells (*BMP*), and BMP-treated cells after transfection with either scrambled siRNA (*Scr siRNA*) or Foxo1 siRNA (*Foxo1 siRNA*) containing vectors (*E*). To overexpress Foxo1, C3H10T1/2 cells were transfected with Foxo1 expression vector (or control vector) for 48 h and increased levels of Foxo1 and Runx2 protein confirmed by Western blot analysis (*F*). Expression of Runx2, ALP, and osteocalcin were measured by semiquantitative RT-PCR (*G*). Values relative to control vector are shown. Data are expressed as means ± S.D. of three experiments. *, significantly different from control ($p < 0.05$); **, significantly different from stimulated control and scrambled siRNA ($p < 0.05$).

siRNA showed markedly less calcium accumulation in the extracellular matrix (Fig. 2*E*), as visualized by alizarin red staining.

The effect of Foxo1 on Runx2 protein levels in nuclear extracts, key osteoblast marker, in the absence of BMP2 stimulation was evaluated by overexpression of Foxo1 in C3H10T1/2

TABLE 1
Effect of Foxo1 siRNA on apoptosis and proliferation

	Apoptosis (+/− S.D.)	Proliferation (+/− S.D.)
	OD[a]	%
Control	143+/−12	200+/−4.8
Scr siRNA	175+/−23	171+/−2.3
Foxo1 siRNA	181+/−31	175+/−5.6

[a] OD, optical density.

cells (Fig. 2*F*). Compared with controls, Foxo1 overexpression also significantly up-regulated the expression of Runx2 (2.2-fold), ALP (2.7-fold), and osteocalcin (4.6-fold) (Fig. 2*G*) ($p < 0.05$).

Silencing of Foxo1 Impairs Normal Skeletogenesis—The expression of Foxo1 was evaluated during active skeletal development, E15.5 (Fig. 3*A*), because this stage has the most ossification centers present in the mouse embryonic skeleton (27). The results demonstrated that Foxo1 is expressed in multiple tissues, *i.e.* brain, tongue, liver, and cartilage, with the highest expression levels in areas of mesenchymal cell differentiation into bone, such as the developing calvaria (7-fold) and diaphysis (7-fold) of long bones. Immunohistochemical staining of these tissues (Fig. 3*B*) confirmed these observations.

Pregnant mice were injected with either Foxo1 miRNA or control miRNA to evaluate the role of Foxo1 on skeletogenesis. The specificity of the Foxo1 miRNA was first tested in C3H10T1/2 cells by EMSA (Fig. 4*A*). Foxo1 expression in calvaria and tibia was silenced 68% (Table 2). Foxo3 and Foxo4 expression did not change with Foxo1 miRNA (Table 2). Whole skeleton staining with alizarin red and Alcian blue showed that silencing Foxo1 impaired skeletal development (Fig. 4*B*). Embryos that received the Foxo1 miRNA lentiviral vector were smaller in size with delayed ossification of supraoccipitale and forelimbs (*arrowheads* in Fig. 4*B*, *panel i*). In addition, in the craniofacial area, the nasal bone, premaxilla, and mandible were on average 20% smaller, which was statistically significant (Fig. 4*B*). Also, in embryos exposed to Foxo1 miRNA, there were 35 and 40% decrease in ossification of the clavicles (Fig. 4*C*) and palatine process (Fig. 4*D*), respectively ($p < 0.05$). The microCT scans of the tibiae from these embryos reveal a 38% decrease in the bone volume fraction, a 12% decrease in the bone mineral density, and a striking 59% decrease in the overall mineral content of the tibiae (Table 2). The three-dimensional reconstruction of microCT data from representative tibiae shows the considerably different appearance of these embryonic bones (Fig. 4*E*).

Foxo1 Regulates Runx2 Expression and Directly Interacts with Runx2—Organ culture was used to examine the Foxo1 mechanism of action on skeleton development. The *ex vivo* culture of developing bones is a versatile three-dimensional model to study the effect of Foxo1 expression/activity on bone formation. Indeed, we found that in comparison with regions that remain cartilaginous (epiphysis) (Fig. 5*A*), the activity of Foxo1 in the areas of active bone formation (diaphysis) was 3.4-fold higher (Fig. 5*B*) and, interestingly, the activity of Runx2 in the same nuclear extracts was 6.7-fold higher (Fig. 5*B*). When mouse embryonic tibiae were incubated with lentivirus expressing Foxo1 miRNA for 48 h, the expression of Foxo1 was

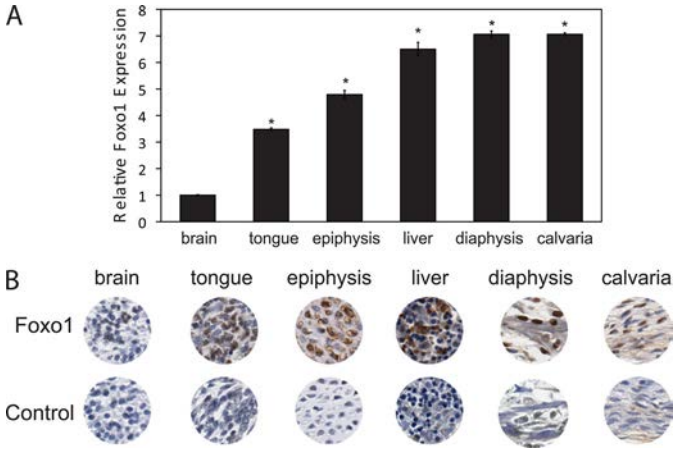

FIGURE 3. **Foxo1 expression is elevated in skeletal tissues during mouse development.** Mouse embryos (E15.5) were collected and mRNA extracted from different tissues for semiquantitative RT-PCR (*A*). Results are presented as Foxo1 expression levels relative to expression in brain. *, significantly different from brain levels ($p < 0.05$). Some embryos were fixed and embedded in paraffin, and sections were used for immunohistochemistry staining with anti-Foxo1 antibody (*Foxo1*) or pre-immune serum (*control*). Foxo1-positive cells are stained brown in different tissues (*B*).

reduced 76%, Runx2 expression decreased 63%, and ALP expression decreased 61% (Fig. 5*C*) in the areas of active bone formation. The histological appearance of tibia exposed to Foxo1 miRNA was also very different from tibia exposed to control miRNA. Silencing of Foxo1 *ex vivo* resulted in shorter (Fig. 5*D*) and less mineralized tibiae as shown by von Kossa staining of the diaphysis of these long bones (Fig. 5*E*).

A luciferase reporter plasmid containing different fragments of the Runx2 promoter was used to investigate the possibility of Foxo1 controlling Runx2 expression. Sequence analysis of the Runx2 promoter suggested the presence of three putative Foxo1 binding sites between −900 to −1300 kb (Fig. 6*A*) and two binding sites below −900 kb region of the promoter. In the first step of screening for potential binding sites, C3H10T1/2 cells were co-transfected with a plasmid containing either Foxo1 or control plasmid, and the Runx2 promoter luciferase plasmid (0.9 or 1.3 kb) for 48 h, in the absence of any osteogenic stimulant. Fig. 6*B* shows that overexpression of Foxo1 in comparison to control plasmid resulted in a statistically significant increase in Runx2 promoter activity ($p < 0.05$) based on luciferase activity (2.7-fold). This effect was observed only with the promoter fragment that included the Foxo1 binding sites between −900 and −1200 kb (1.2-kb fragment). To further characterize the binding sites in the region between −900 and −1300 kb, three potential sequences were identified (Fig. 6*A*), and three synthetic oligonucleotide were created. (probes A, B, and C) for EMSA, encompassing these three regions. EMSA results demonstrated that probes A and B had the ability to

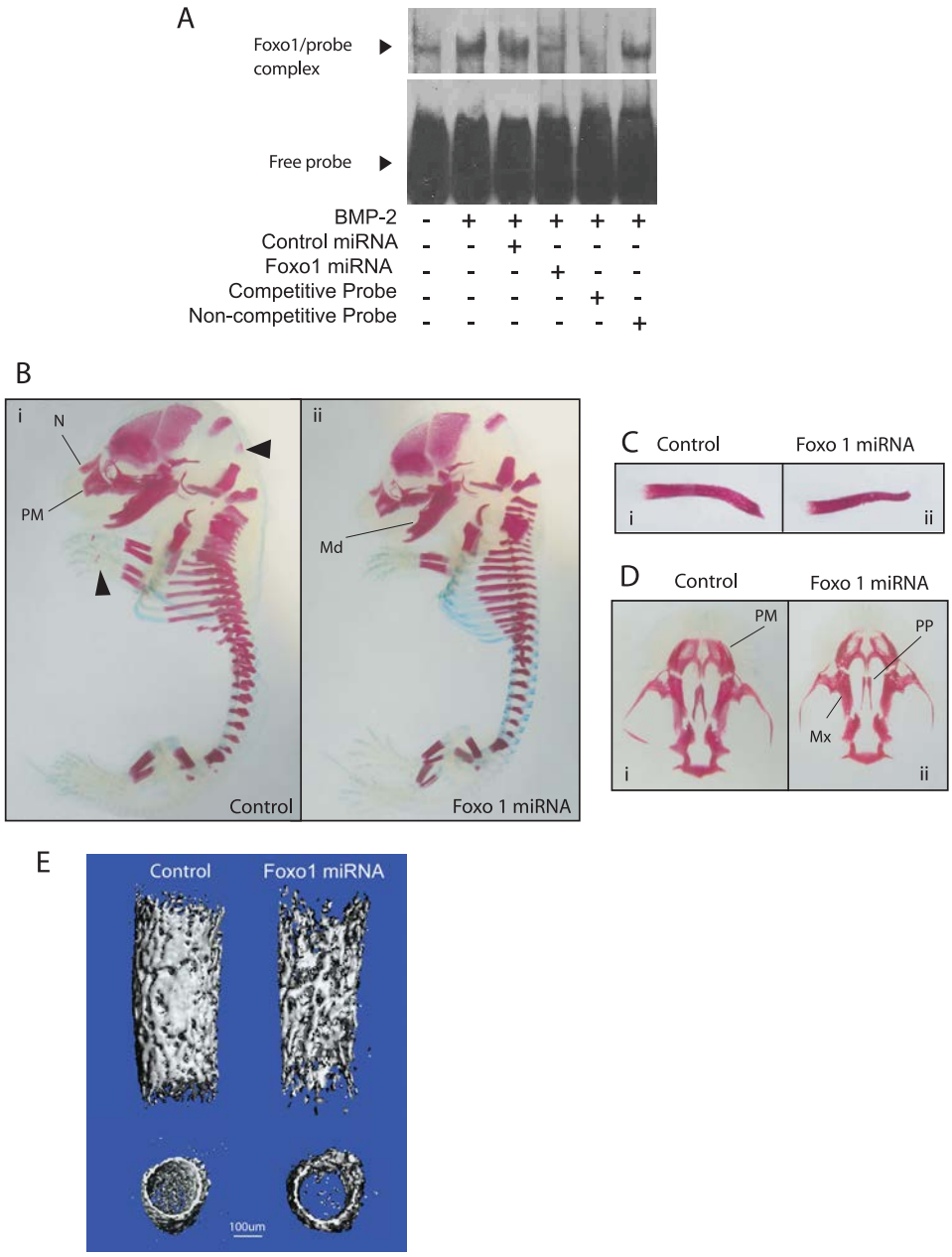

FIGURE 4. **Silencing Foxo1 impairs skeletal development in mouse embryos.** Foxo1 miRNA silencing specificity was evaluated by EMSA in C3H10T1/2 cells infected with Foxo1 miRNA or control miRNA lentiviral vectors (48 h) and stimulated with BMP2 (100 ng/ml) for 24 h (*A*). Foxo1 expression was reduced *in vivo*, by tail vein injection of pregnant mice (E14.5) with these lentiviral vectors. Skeletons of E16.5 embryos were stained with alizarin red and Alcian blue. *B*, note the overall decrease in size of skeletal structures in experimental animals (*ii*) compared with control (*i*). *Black arrowheads* show additional ossification centers in control animals (*i*). *C*, clavicles from control (*i*) and experimental embryos (*ii*) were photographed side by side. *D*, *axial view* of cranial bones from control (*i*) and experimental (*ii*) embryos after removing cranial vault structures are shown (*Md* = mandible, *n* = nasal bone, *PM* = pre-maxilla, *Mx* = maxilla, *PP* = palatine process). Tibiae from experimental and control embryos were analyzed by microCT and 3D images created (*E*).

TABLE 2

Effect of Foxo1 miRNA on developing tibia

Bone volume fraction (BVF), bone mineral density (BMD), and total mineral content (Min Cont) were determined by microCT. Expression of Foxo1 (Foxo 1 exp), Foxo3 (Foxo 3 exp), and Foxo4 (Foxo 4 exp) measured by semiquantitative RT-PCR in tibiae infected with Foxo1 miRNA viral vector is presented relative to levels in tibiae infected with control miRNA vector. Data are expressed as means ± S.D. of three experiments.

	Control	Foxo 1 miRNA
Foxo 1 exp	1	0.32 ± 0.06[a]
Foxo 3 exp	1	1.2 ± 0.24
Foxo 4 exp	1	1.3 ± 0.26
BVF (%)	13.7 ± 1.87	8.54 ± 0.94[a]
BMD (mg/cc)	263.1 ± 18.27	232.3 ± 15.54[a]
Min Cont (μg)	5.6 ± 1.4	2.3 ± 0.8[a]

[a] Significantly different from control miRNA values ($p < 0.05$).

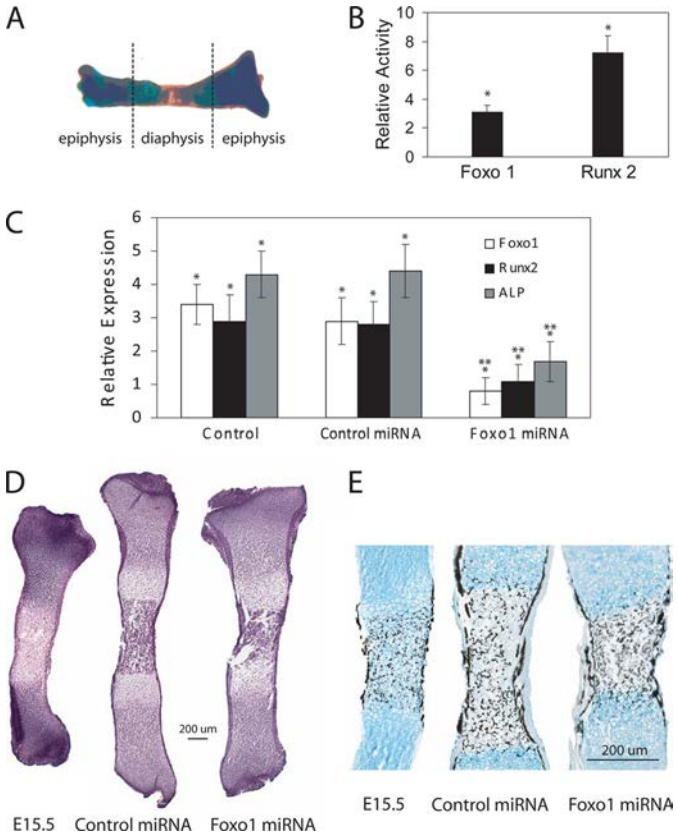

FIGURE 5. **Silencing Foxo1 expression in tibia organ culture reduces osteoblast markers and bone growth.** The cartilaginous epiphysis and bone forming region of the diaphysis of E15.5 mouse tibia (*A*) (cartilage stained with Alcian blue, bone stained with alizarin red) were dissected. Runx2 and Foxo1 activity levels were measured (*B*). Data are shown as activity levels in diaphysis relative to the epiphysis. *, significantly different from epiphysis ($p < 0.05$). In parallel experiments, tibiae were infected with either miRNA Foxo1 or control miRNA lentiviral vectors or no vector at all (control). Two days later tibiae were collected, mRNA was extracted from the two regions (epiphysis and diaphysis), and expression levels of Foxo1, Runx2, and alkaline phosphatase (ALP) were determined by semiquantitative RT-PCR (*C*). Data are shown as expression levels in diaphysis relative to the epiphysis. *, significantly different from epiphysis; **, significantly different from control and control miRNA ($p < 0.05$). Some tibiae were also fixed and embedded in paraffin, and sections were stained with hematoxylin & eosin (*D*) or von Kossa and Alcian blue (*E*) to visualize mineralization of the bone forming region of the diaphysis. Histological images of tibia collected at the initiation of the experiments are also shown (E15.5).

compete with the labeled probe, whereas probe C produced only partial competition (Fig. 6*C*). Additionally, four base mutations introduced into the putative binding sites A, B, and C, and the Runx2 promoter activity in response to Foxo1 overexpression was reduced 92%, 89 and 74%, respectively (Fig. 6*D*).

A ChIP assay was used to investigate if Foxo1 binds directly to the Runx2 promoter. C3H10T1/2 cells were treated with BMP2 for 48 h, and their chromatin was immunoprecipitated overnight with either anti-Foxo1 antibody or normal rabbit IgG. Immunoprecipitates were analyzed by Western blot using anti-Foxo1 antibody (Fig. 6*E*). The PCR analysis using specific primers flanking the putative Foxo1 binding sites in the Runx2, ALP, or osteocalcin promoter showed a 14.2-fold (Fig. 6*F*), 2.7-fold (Fig. 6*G*), and 9-fold (Fig. 6*H*) increase in the expression of these markers in the Foxo1 precipitates when compared with the IgG control. Analysis of promoter sequences of numerous osteoblast markers (Biobase, Biological Databases, Beverly, MA) revealed the presence of both Foxo1 and Runx2 putative binding sites in close proximity (<100 bp) (data not shown) suggesting the possibility of direct interaction between these two transcription factors and cooperation during transcriptional regulation of osteoblast differentiation. To investigate this possibility, we conducted co-immunoprecipitation experiments. Note the increase in Runx2 protein in the immunoprecipitates using anti-FLAG antibody (Fig. 6*I*, *left panel*) and Foxo1 protein in the immunoprecipitates using anti-Runx2 antibody (Fig. 6*I*, *right panel*). To eliminate the possibility of nonspecific interaction between Foxo1 and Runx2 due to overexpression of Foxo1, immunoprecipitation experiments were also performed using MC3T3-E1 cells treated with BMP2 (Fig. 6*J*). Results were in agreement with immunoprecipitation after Foxo1 overexpression in C3H10T1/2 and support the direct interaction between these transcription factors.

To further validate the cooperation of these 2 transcription factors in gene regulation Foxo1 and Runx2 were co-transfected into mesenchymal cells (Fig. 6*K*). Although the transfection with either Foxo1 or Rux2 resulted in an increase osteocalcin expression level as measured by RT-PCR (3.8- and 6.4-fold, respectively), a synergistic response resulting in an 18-fold increase in expression was observed in the presence of these two transcription factors (statistically significant, $p < 0.05$).

DISCUSSION

The Foxo subfamily of forkhead box transcription factors regulates expression of genes in a variety of physiological events, but their role in growth and development, specifically on skeletogenesis, is not well characterized. In this investigation, using different methods and models we have defined a new and important function for Foxo1 in skeletal development.

It has been previously reported that Foxo1 is expressed in different tissues, such as brain (28), heart (29, 30), liver (29, 30), lung (31, 32), muscle (33), and fat (18). Here, we show that, during embryonic development, Foxo1 is expressed at its highest level in the areas of intramembranous bone formation, such as calvaria, and endochondral bone formation, such as the diaphysis of long bones.

Foxo1 knock-out animals would be ideal to evaluate the effect of Foxo1 on skeletogenesis, but these animals do not survive past E10.5–11, which is before osteoblast differentiation (34, 35) occurs. Because Foxo1 have a wide variety of roles, early conditional knock-out in mesenchymal cells could nonspecifically disturb developmental process. Also conditional knock-out mice in specific cell types, such as osteoblasts, will not determine early events before differentiation of mesenchymal cells into osteoblasts. As a consequence, our strategy was to down-regulate Foxo1 expression/activity around the time of active skeletogenesis in developing embryos using microRNA technology delivered through a lentivirus, to avoid disturbing other developmental processes. Recent work on animal gene therapy has demonstrated extensive gene silencing at the tissue level (36, 37), which supports the use of lentivirus and miRNA as a powerful tool for silencing *in vivo* models and even non-dividing cells (38). Similarly, our finding suggests a potential usage for miRNA in developmental biology studies.

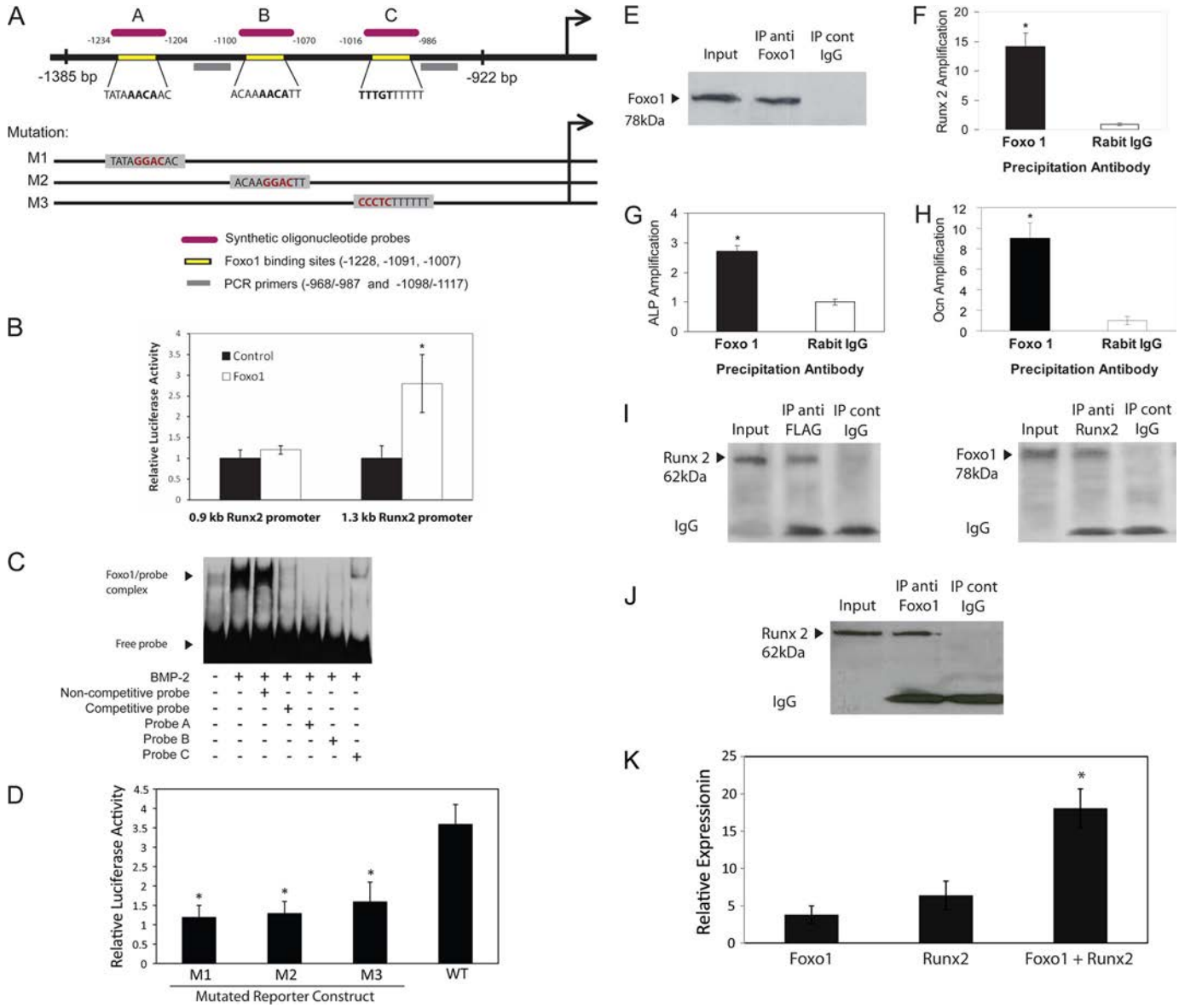

FIGURE 6. **Foxo1 regulates Runx2 promoter activity, binds to the promoter of Runx2, ALP, and Osteocalcin genes, and directly interacts with Runx2 protein.** Shown are the schematic of potential Foxo1 binding sites in the Runx2 promoter, position of synthetic oligonucleotide probes, PCR primer location, and mutations in three Foxo1 binding sites (*A*). C3H10T1/2 cells were co-transfected for 48 h with a plasmid containing either Foxo1 or control plasmid, and Runx2 promoter luciferase plasmid (containing a 0.9- or 1.3-kb promoter fragment), in the absence of any osteogenic stimulant (*B*). Data are presented as a ratio of experimental/control luciferase. Values relative to control vector are shown. *, significantly different from control ($p < 0.05$). Activation of Foxo1 was measured by EMSA after C3H10T1/2 stimulation with BMP2 (100 ng/ml) for 24 h, using competitive DNA probes A, B, and C. *C*, unlabeled Foxo1 in excess was used as a competitive inhibitor. A probe with a nonspecific sequence was used as non-competitive probe. Runx2 promoter luciferase constructs carrying a four-base mutation in Foxo1 binding sites (*M1*, *M2*, and *M3*) were used to measure promoter activity in response to Foxo1 overexpression (*D*). Data are presented as a ratio of experimental/control luciferase. Values relative to control vector are shown. Data are expressed as means ± S.D. of three experiments. *, significantly different from wild-type (*WT*) construct ($p < 0.05$). Foxo1 protein binding to the Runx2, ALP, and osteocalcin promoter was evaluated using ChIP assay. C3H10T1/2 cells were treated with BMP2 (100 ng/ml) for 48 h. Chromatin was immunoprecipitated with either anti-Foxo1 antibody or normal rabbit IgG as control. Western analysis of immunoprecipitates was performed using anti-Foxo1 antibody (*E*). DNA from each immunoprecipitation reaction was examined by real-time PCR using specific primers flanking the putative Foxo1 binding site in the Runx2 (*F*) or ALP (*G*) or Osteocalcin (*H*) promoters. Results are presented as amplification levels in relation to IgG control precipitates. Data are expressed as means ± S.D. of three experiments. *, significantly different from IgG control ($p < 0.05$). Nuclear extracts of C3H10T1/2 cells that have been transfected with pcDNA3 FLAG Foxo1 and treated with BMP2 (100 ng/ml) were immunoprecipitated (*IP*) with an anti-FLAG, anti-Runx2, or with nonspecific IgG antibodies. Immunoprecipitated complexes were analyzed by Western blotting with anti-Runx2 (*left panel*) or anti-Foxo1 (*right panel*) antibodies (*I*). In similar experiments, MC3T3-E1 cells were treated with BMP2 (100 ng/ml) and nuclear extracts were immunoprecipitated with anti-Foxo1 or with nonspecific IgG antibodies. Immunoprecipitated complexes were analyzed by Western blotting with anti-Runx2 antibody (*J*). C3H10T1/2 cells were transfected for 48 h with a plasmid containing Foxo1, Runx2, or control plasmid. Some cells were co-transfected with a Foxo1 and Runx2 plasmid. Expression of osteocalcin was measured by semiquantitative RT-PCR (*K*). Values relative to control vector are shown. Data are expressed as means ± S.D. of three experiments. *, significantly different from Foxo1 or Runx2 alone ($p < 0.05$) (*I*).

Because Foxo1 null mice show embryonic lethality and defects in the formation of the vascular system of the embryo and yolk sac (34, 35), it can be argued that silencing Foxo1 indirectly affects skeletogenesis through its impact on angiogenesis. Although this possibility cannot be ruled out, the short duration of our silencing approach and our *in vitro* and *ex vivo* results supports the direct contribution of Foxo1 in skeletogenesis.

Previously, we and others have demonstrated that Foxo1 may play a role in apoptosis (39, 40) or cell cycle progression (41). The effect of Foxo1 on proliferation and apoptosis was studied at *in vitro* and *in vivo* levels to demonstrate that the mechanism through which silencing Foxo1 impairs skeletogenesis is not related to these events. At the *in vitro* level Foxo1 silencing or overexpression did not have a significant effect on apoptosis or proliferation of osteoblasts in comparison with scrambled siRNA. Similarly, embryos infected with Foxo1 miRNA did not demonstrate higher apoptosis in comparison with embryos that received control miRNA. This is consistent with a recent study that demonstrated Foxo1 conditional knock-out mice did not show any adverse effect on apoptosis or proliferation (42). Therefore, we conclude that it is possible for Foxo1 to affect skeletogenesis through a direct role in the differentiation of osteoblasts.

Our *in vitro* findings demonstrate that Foxo1 is critical during BMP2-induced differentiation of mice mesenchymal cells into osteoblasts. Although it cannot be ruled out that a percentage of these cells under BMP-2 stimulation can differentiate into chondroblasts (43), at the cell densities used and the duration of our study (1 week) the expression of collagen type II (chondrogenic marker) did not change significantly, which argues in favor of activation of the osteogenic pathway.

Foxo1 activity is detected *in vitro* shortly after stimulation of mesenchymal cells with SHH (25), or PTHrP (26), which suggests that Foxo1 activity is stimulated by other osteogenic agents in addition to BMP2. Activation of Foxo1 during differentiation of MC3T3-E1 cells in response to ascorbic acid and β-glycerophosphate or primary human mesenchymal cells in response to dexamethasone demonstrates that activation of Foxo1 is not an isolated phenomenon tied to a specific cell line.

Runx2 has been shown to play a critical role in osteoblast differentiation (44–46). In this study we demonstrate that Foxo1 directly interacts with Runx2 promoter through at least three DNA binding sites and regulates its expression. The observation that Foxo1 protein levels and activity were detected earlier than Runx2 expression supports the model that Foxo1 activation is positioned as an upstream event in Runx2-mediated osteoblast differentiation. This is in agreement with our *in vivo* findings that demonstrated silencing of Foxo1 during embryonic bone formation had a significant impact on many skeletal elements, including long bones, clavicles, and bones in the craniofacial area, which mimic, to some extent, the skeletal abnormalities found in mice heterozygous for the Runx2 mutation (45). This phenotype is similar to the cleidocranial dysplasia syndrome observed in humans. It should be emphasized that the effect of silencing Foxo1 on skeletogenesis can be due in part to a direct effect on chondrocyte differentiation or maturation, which has not been addressed in this report. Our current work explores this possibility.

Although these data place Foxo1 upstream of Runx2 signaling, the co-immunoprecipitation results, together with the promoter sequence analysis of numerous osteogenic factors and osteoblast marker genes, and the synergic effect of Foxo1 and Runx2 on osteocalcin expression, strongly support the possibility of cooperation between these two transcription factors during osteoblast differentiation. Indeed, recent work (42) showing that osteocalcin promoter has binding sites for both Runx2 and Foxo1 argues in favor of functional interaction between Foxo1 and Runx2. Further functional analysis to clarify the nature of this interaction is necessary. However, Foxo1 may also control osteoblast differentiation through direct regulation of osteogenic genes such as ALP (15). The presence of binding sites only for Foxo1 in the promoters of some of these genes argues in favor of a Runx2-independent effect of Foxo1.

Recently, it has been shown that Foxo1 represses peroxisome proliferator-activated receptor-γ, and through this mechanism prevents the differentiation of preadipocytes (16–18, 30, 31). Similarly, the expression of constitutively active Foxo1 decreases myoblast differentiation (30) and reduces muscle mass in transgenic mice (49). Our data suggests that Foxo1 drives mesenchymal cells toward osteogenic differentiation by up-regulating the expression of osteogenic markers. Taken together, these studies suggest a role for Foxo1 as an early molecule in determining the destiny of mesenchymal cells. The role of Foxo1 in differentiation of osteoblasts also can explain the mechanism of BMP2 inhibition of normal adipocyte differentiation and concurrent stimulation of the osteogenic pathway (50).

It has been shown that bone marrow at a very early age is virtually devoid of adipocytes, whereas with aging, a decrease in bone volume occurs with a reciprocal increase in fat deposits within the marrow (observed, *e.g.* in age-related osteopenia) (51–53). Because the adult organism does not possess a large population of mesenchymal cells (54–56), understanding the pathway controlling the balance between bone formation and adipogenesis can lead to the development of novel therapeutic approaches in the prevention or treatment of conditions characterized by inadequate bone formation and excessive marrow adipogenesis. In addition, controlling the commitment and differentiation of mesenchymal cells into osteoblasts is also of considerable interest for enhancement of bone formation in a myriad of clinical situations, including bone repair, treatment of non-unions, and maintenance of bone mass during aging.

REFERENCES

1. Grigoriadis, A. E., Heersche, J. N., and Aubin, J. E. (1988) *J. Cell Biol.* **106,** 2139–2151
2. Mundlos, S., Otto, F., Mundlos, C., Mulliken, J. B., Aylsworth, A. S., Albright, S., Lindhout, D., Cole, W. G., Henn, W., Knoll, J. H., Owen, M. J., Mertelsmann, R., Zabel, B. U., and Olsen, B. R. (1997) *Cell* **89,** 773–779
3. Kaestner, K. H., Knochel, W., and Martinez, D. E. (2000) *Genes Dev.* **14,** 142–146
4. Guo, S., Rena, G., Cichy, S., He, X., Cohen, P., and Unterman, T. (1999) *J. Biol. Chem.* **274,** 17184–17192
5. Nakae, J., Barr, V., and Accili, D. (2000) *EMBO J.* **19,** 989–996
6. Biggs, W. H., 3rd, Meisenhelder, J., Hunter, T., Cavenee, W. K., and Arden, K. C. (1999) *Proc. Natl. Acad. Sci. U.S.A.* **96,** 7421–7426
7. Tang, E. D., Nuñez, G., Barr, F. G., and Guan, K. L. (1999) *J. Biol. Chem.* **274,** 16741–16746
8. Jackson, J. G., Kreisberg, J. I., Koterba, A. P., Yee, D., and Brattain, M. G. (2000) *Oncogene* **19,** 4574–4581
9. Nasrin, N., Ogg, S., Cahill, C. M., Biggs, W., Nui, S., Dore, J., Calvo, D., Shi, Y., Ruvkun, G., and Alexander-Bridges, M. C. (2000) *Proc. Natl. Acad. Sci. U.S.A.* **97,** 10412–10417
10. Birkenkamp, K. U., and Coffer, P. J. (2003) *J. Immunol.* **171,** 1623–1629
11. Peng, S. L. (2007) *Autoimmunity* **40,** 462–469
12. Lam, E. W., Francis, R. E., and Petkovic, M. (2006) *Biochem. Soc. Trans.* **34,**

722–726
13. Maiese, K., Chong, Z. Z., and Shang, Y. C. (2008) *Trends Mol. Med.* **14,** 219–227
14. van der Vos, K. E., and Coffer, P. J. (2008) *Oncogene* **27,** 2289–2299
15. van der Horst, A., and Burgering, B. M. (2007) *Nat. Rev. Mol. Cell Biol.* **8,** 440–450
16. Gilde, A. J., and Van Bilsen, M. (2003) *Acta Physiol. Scand.* **178,** 425–434
17. Armoni, M., Harel, C., Karni, S., Chen, H., Bar-Yoseph, F., Ver, M. R., Quon, M. J., and Karnieli, E. (2006) *J. Biol. Chem.* **281,** 19881–19891
18. Nakae, J., Kitamura, T., Kitamura, Y., Biggs, W. H., 3rd, Arden, K. C., and Accili, D. (2003) *Dev. Cell* **4,** 119–129
19. Hatta, M., Daitoku, H., Matsuzaki, H., Deyama, Y., Yoshimura, Y., Suzuki, K., Matsumoto, A., and Fukamizu, A. (2002) *Int. J. Mol. Med.* **9,** 147–152
20. Jaiswal, N., Haynesworth, S. E., Caplan, A. I., and Bruder, S. P. (1997) *J. Cell Biochem.* **64,** 295–312
21. Serra, R., Karaplis, A., and Sohn, P. (1999) *J. Cell Biol.* **145,** 783–794
22. Teixeira, C. C., Ischiropoulos, H., Leboy, P. S., Adams, S. L., and Shapiro, I. M. (2005) *Bone* **37,** 37–45
23. Ahrens, M., Ankenbauer, T., Schroder, D., Hollnagel, A., Mayer, H., and Gross, G. (1993) *DNA & Cell Biol.* **12,** 871–880
24. Wang, E. A., Israel, D. I., Kelly, S., and Luxenberg, D. P. (1993) *Growth Factors* **9,** 57–71
25. Yamaguchi, A., Komori, T., and Suda, T. (2000) *Endocr. Rev.* **21,** 393–411
26. Chen, H. L., Demiralp, B., Schneider, A., Koh, A. J., Silve, C., Wang, C. Y., and McCauley, L. K. (2002) *J. Biol. Chem.* **277,** 19374–19381
27. Karsenty, G. (1999) *Genes Dev.* **13,** 3037–3051
28. Polter, A., Yang, S., Zmijewska, A. A., van Groen, T., Paik, J. H., Depinho, R. A., Peng, S. Nakae, J., Kitamura, T., Silver, D. L., Jope, R. S., and Li, X. (2009) *Biol. Psychiatry* **65,** 150–159
29. Ropelle, E. R., Pauli, J. R., Prada, P., Cintra, D. E., Rocha, G. Z., Moraes, JC., Frederico, M. J., da Luz, G., Pinho, R. A., Carvalheira, J. B., Velloso, L. A., Saad, M. A., and De Souza, C. T. (2009) *J. Physiol.* **587,** 2341–2351
30. Li, T., Kong, X., Owsley, E., Ellis, E., Strom, S, and Chiang, J. Y. (2006) *J. Biol. Chem.* **281,** 28745–28754
31. Nakae, J., Kitamura, T., Silver, D. L., and Accili, D. (2001) *J. Clin. Invest.* **108,** 1359–1367
32. Kitamura, T., Nakae, J., Kitamura, Y., Kido, Y., Biggs, W. H., 3rd, Wright, C. V., White, M. F., Arden, K. C., and Accili, D. (2002) *J. Clin. Invest.* **110,** 1839–1847
33. Yasui, A., Nishizawa, H., Okuno, Y., Morita, K., Kobayashi, H., Kawai, K., Matsuda, M., Kishida, K., Kihara, S., Kamei, Y., Ogawa, Y., Funahashi, T., and Shimomura, I. (2007) *Biochem. Biophys. Res. Commun.* **364,** 358–365
34. Furuyama, T., Kitayama, K., Shimoda, Y., Ogawa, M., Sone, K., Yoshida-Araki, K., Hisatsune, H., Nishikawa, S., Nakayama, K., Ikeda, K., Motoyama, N., and Mori, N. (2004) *J. Biol. Chem.* **279,** 34741–34749
35. Hosaka, T., Biggs, W. H., 3rd, Tieu, D., Boyer, A. D., Varki, N. M., Cavenee, W. K., and Arden, K. C. (2004) *Proc. Natl. Acad. Sci. U.S.A.* **101,** 2975–2980
36. Gratsch, T. E., De Boer, L. S., and O'Shea, K. S. (2003) *Genesis* **37,** 12–17
37. Franceschi, R. T., Yang, S., Rutherford, R. B., Krebsbach, P. H., Zhao, M., and Wang, D. (2004) *Cells Tissues Organs* **176,** 95–108
38. Scherr, M., and Eder, M. (2007) *Cell Cycle* **6,** 444–449
39. Alikhani, M., Maclellan, C. M., Raptis, M., Vora, S., Trackman, P. C., and Graves, D. T. (2007) *Am. J. Physiol. Cell Physiol.* **292,** C850–856
40. Alikhani, M., Alikhani, Z., and Graves, D. T. (2005) *J. Biol. Chem.* **280,** 12096–12102
41. Greer, E. L., and Brunet, A. (2005) *Oncogene* **24,** 7410–7425
42. Rached, M. T., Kode, A., Silva, B. C., Jung, D. Y., Gray, S., Ong, H., Paik, J. H., DePinho, R. A., Kim, J. K., Karsenty, G., and Kousteni, S. (2010) *J. Clin. Invest.* **120,** 357–368
43. Shea, C. M., Edgar, C. M., Einhorn, T. A., and Gerstenfeld, L. C. (2003) *J. Cell Biochem.* **90,** 1112–1127
44. Ducy, P., Zhang, R., Geoffroy, V., Ridall, A. L., and Karsenty, G. (1997) *Cell* **89,** 747–754
45. Otto, F., Thornell, A. P., Crompton, T., Denzel, A., Gilmour, K. C., Rosewell, I. R., Stamp, G. W., Beddington, R. S., Mundlos, S., Olsen, B. R., Selby, P. B., and Owen, M. J. (1997) *Cell* **89,** 765–771
46. Komori, T., Yagi, H., Nomura, S., Yamaguchi, A., Sasaki, K., Deguchi, K., Shimizu, Y., Bronson, R. T., Gao, Y. H., Inada, M., Sato, M., Okamoto, R., Kitamura, Y., Yoshiki, S., and Kishimoto, T. (1997) *Cell* **89,** 755–764
47. Hribal, M. L., Nakae, J., Kitamura, T., Shutter, J. R., and Accili, D. (2003) *J. Cell Biol.* **162,** 535–541
48. Allen, D. L., and Unterman, T. G. (2007) *Am. J. Physiol. Cell Physiol.* **292,** C188–199
49. Kamei, Y., Miura, S., Suzuki, M., Kai, Y., Mizukami, J., Taniguchi, T., Mochida, K., Hata, T., Matsuda, J., Aburatani, H., Nishino, I., and Ezaki, O. (2004) *J. Biol. Chem.* **279,** 41114–41123
50. Skillington, J., Choy, L., and Derynck, R. (2002) *J. Cell Biol.* **159,** 135–146
51. Gimble, J. M., Zvonic, S., Floyd, Z. E., Kassem, M., and Nuttall, M. E. (2006) *J. Cell Biochem.* **98,** 251–266
52. Nuttall, M. E., and Gimble, J. M. (2004) *Curr. Opin. Pharmacol.* **4,** 290–294
53. Nuttall, M. E., and Gimble, J. M. (2000) *Bone* **27,** 177–184
54. Friedenstein, A. J., Chailakhyan, R. K., and Gerasimov, U. V. (1987) *Cell Tissue Kinet* **20,** 263–272
55. Nakashima, K., Zhou, X., Kunkel, G., Zhang, Z., Deng, J. M., Behringer, R. R., and de Crombrugghe, B. (2002) *Cell* **108,** 17–29
56. Owen, M. E., Cavé, J., and Joyner, C. J. (1987) *J. Cell Sci.* **87,** 731–738